Effects of operating condition variations on vibration-based bearing condition monitoring features: Experimental investigation

Agusmian Partogi Ompusunggu, Steven Devos

Flanders Make vzw, Celestijnenlaan 300, Leuven, 3001 Belgium
agusmian.ompusunggu@flandersmake.be
steven.devos@flandersmake.be

ABSTRACT

The envelope spectrum analysis on vibration signals has been demonstrated for many years as a powerful technique to extract effective indicators (features) for condition monitoring of rolling element bearings under stationary operating conditions. As will be shown in this paper, applying these diagnostic features without a care to rotating machines subject to varying operating conditions may lead to unreliable bearing fault diagnostics. Hence, the applicability of the diagnostic features is rather limited. To extend the applicability of the diagnostic features, number of researchers/research institutes have developed new features/methods to deal with variation of operating conditions. However, the methods proposed in the literature mainly focuses on shaft speed variations. In practice, both shaft speed and load can vary in time simultaneously so there might be an interaction effect on the diagnostic features responses. Moreover, the bearing temperature, being an operational parameter, may also vary significantly in some applications. Because the temperature affects the film thickness formed between the rolling elements and the raceways of bearings, which in turn contributes to the damping and contact stiffness of bearings, it is believed that the bearing temperature might also play an important role on the diagnostic features responses. To improve our understanding on how the three operational parameters variations, namely speed, load and temperature, affect the diagnostic feature responses, a set of experiments has been designed to investigate the effects using an in-house developed test setup. The main effects of the operational parameters on the diagnostic features are presented and discussed in this paper. Qualitative models describing the relationships between the diagnostic features and the operational parameters are deduced and discussed in the

paper. It is believed that these qualitative models can be useful to inspire us in the future to develop methods/strategies for bearing fault diagnostics under varying rotational speed, load and temperature.

1. INTRODUCTION

As one of the most critical elements in rotating machinery, the development of robust and automated bearing fault diagnostics methods using vibration signals has been continuously attracting the attention of many researchers/practitioners for decades.

One of the most successful methods for bearing fault diagnostics is based on the envelope spectrum analysis (Randall & Antoni, 2011). Various approaches to extract bearing fault features automatically from the envelope spectra have been proposed and reported in the literature (Gelman et al., 2013; Ompusunggu et al., 2016; Barbini, et al., 2016). These published papers show that the bearing fault features extracted from the envelope spectra are very effective for distinguishing between a healthy bearing and a faulty bearing under the same operating conditions.

Often, a main bottleneck for companies to fully exploit these innovative diagnostic methods, is the lack of confidence that these – more complex - methods allow to detect faults earlier or more accurately than state of practice solutions. Most often, the relevant data measured on real machines on which bearing faults are occurring, are not immediately available for evaluating the diagnostic methods. Furthermore, for machines operating in many different operating conditions (in particular speed, load and temperature), relevant data obtained from a broad range of operating conditions are needed in order to gain confidence by validating the methods for a given application.

A number of works investigating the effects of different operating conditions (i.e. different speeds and loads) on features extracted from vibration signals of healthy and

faulty bearings have been published. Bartelmus and the co-authors (Bartelmus, & Zimroz, 2009; Zimroz et al. , 2014) used a first order polynomial function to relate the extracted features with the operational parameter (to form a feature-operating condition space). The polynomial coefficients are then used as new features for bearing fault diagnostics. In (Boskoski et al., 2010), features based on the wavelet transformation and the spectral kurtosis were extracted from vibration signals of a gearbox with healthy and faulty bearings under different speed and load conditions. The latter publication shows that the features are influenced by the operating conditions.

To the authors' knowledge, a profound understanding the effects of different operating conditions on envelope-based bearing fault features is still very limited. In this paper, the authors want to clarify the dependency of the enveloped-based diagnostic feature value on different stationary operating conditions (speed, load and temperature), and furthermore evaluate whether this dependency further depends on fault severity. Understanding of these relations will allow us to select the most appropriate features for a particular application and limit the amount of data that is needed for validation.

This paper is structured as follows. Section 2 presents an algorithm based on enhancing envelope spectrum to extract bearing fault feature for specific fault types. Section 3 discusses the experimental methodology. Section 4 discusses the analysis results. Section 5 concludes the paper and discusses some perspectives.

2. BEARING FAULT FEATURE CALCULATION

The bearing fault diagnostics algorithm proposed in this paper is summarized in the flowchart shown in Figure 1. Firstly, discrete components, which are typically dominant in vibration signals of rotating machinery, are removed from the raw signal by the phase-editing method described in (Barbini, et al., 2016). These discrete components are originated from gear-related signals and/or EMI-related signals. Secondly, the filtered signal containing bearing-related information is then subsequently enhanced by the spectral subtraction (SS) and minimum entropy deconvolution (MED). The spectral subtraction aims at reducing random noise from measurements, while the MED filtering aims at enhancing the impulsiveness of the bearing-related signal if present. Finally, bearing fault features are then calculated from the squared envelope spectrum (SES) of the enhanced signal (Randall & Antoni, 2011).

The bearing fault feature F is defined as the summation of the normalized SES magnitudes $\overline{SES}$ of the first five harmonics of a bearing fault frequency of interest ν_b. This definition can be formulated in the following equation:

$$F = \sum_{k=1}^{5} \overline{SES}[k\nu_b] \qquad (1)$$

The normalised SES magnitude $\overline{SES}$ is expressed in the following equation:

$$\overline{SES}[k] = SES[k]/SES[0] \qquad (2)$$

with $SES[0]$ denoting the magnitude of SES at frequency zero.
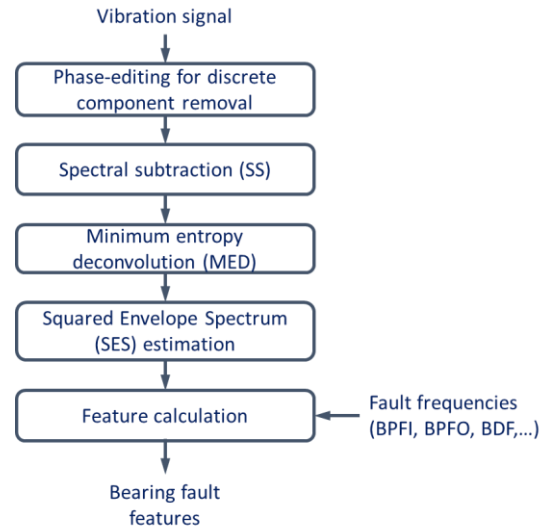

Figure 1. Flowchart of the bearing fault features calculation

3. EXPERIMENT

3.1. Test setup

Figure 2(a) and (b) show the overview and zoomed-in photograph of the bearing setup at Flanders Make. The bearing under test (1) is driven by a speed controlled motor. Its outer ring is supported by a hub. A radial force can be applied to the tested bearing via the hub by means of a hydrostatic pad (2) and pneumatic muscle (3) with a minimal parasitic torque. The frictional force reacting on the outer ring is measured by means of the force cell (4). This frictional force can be used further to estimate the energy consumption of the bearing. The oil is circulated through the bearing and its temperature can be varied by controlling the temperature in the oil tank (not shown in the figure). The bearing temperature is measured by means of temperature sensors (5). An accelerometer is placed in the load zone to measure the acceleration response of the bearing system. Note that the measuring direction of the accelerometer is in parallel with the applied radial load direction.
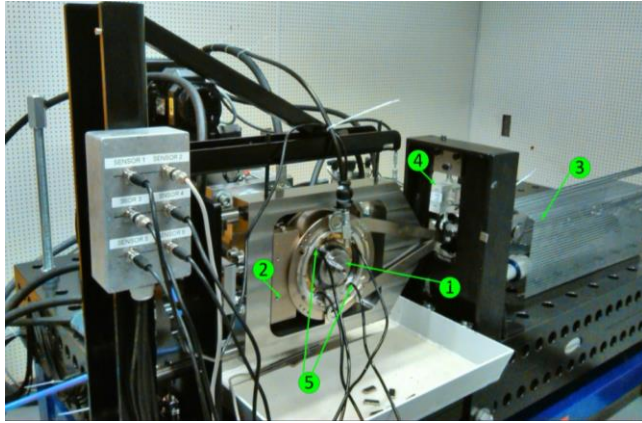
(a)
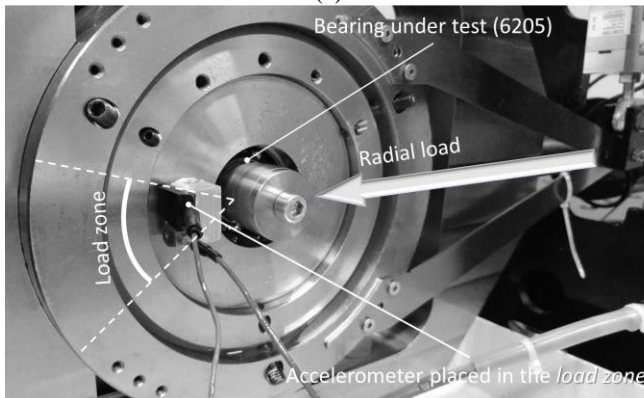
(b)

Figure 2. (a) The overview photograph of the bearing setup (b) the zoomed-in photograph showing the loading condition and the accelerometer position.

3.2. Bearing under test

The bearing type of **6205-C-TVH** was selected in this study. The main criterion for the selection was because this bearing type is relatively easy to be disassembled and reassembled. This criterion is important for inducing faults on the bearings that will be discussed later on in the following paragraphs.

The selected bearing type is a ball bearing having the specifications shown in Figure 3. Based on the geometrical data shown in the figure, the theoretical bearing fault frequencies, like (*i*) ball-pass frequency outer (*BPFO*), (*ii*) ball damage frequency (*BDF*) and (*iii*) ball-pass frequency inner (*BPFI*), can be calculated using the well-known kinematic equations. The equations can be found for example in (Randall & Antoni, 2011). The theoretical fault frequencies of the selected bearing at the shaft speed of 60 rpm are shown in Table 1.
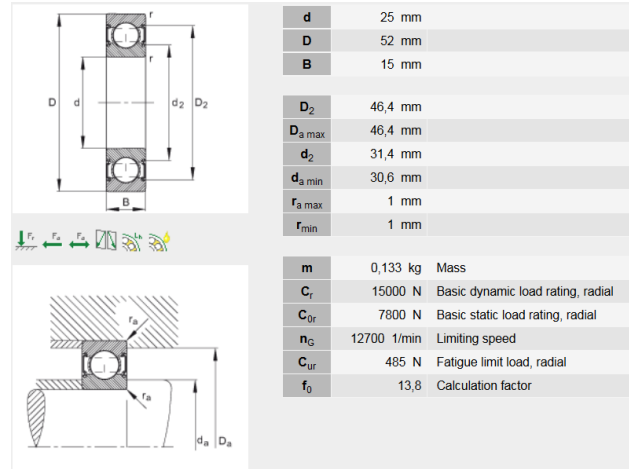

Figure 3. The specifications of the selected bearing type (Source: FAG).

Fault frequency	Value [Hz]
BPFO	3.59
BDF	4.71
BPFI	5.41

Table 1. The theoretical fault frequencies of the 6205-C-TVH bearing at the shaft speed of 60 rpm.

Three bearings of the selected type were used in the experiment. One brand-new bearing was used to represent a healthy bearing. While the other two bearings were induced with realistic spall faults on the inner race with different sizes to represent faulty bearings at different severity levels. Figure 4 shows the optical images of the two bearings induced with realistic spall faults.
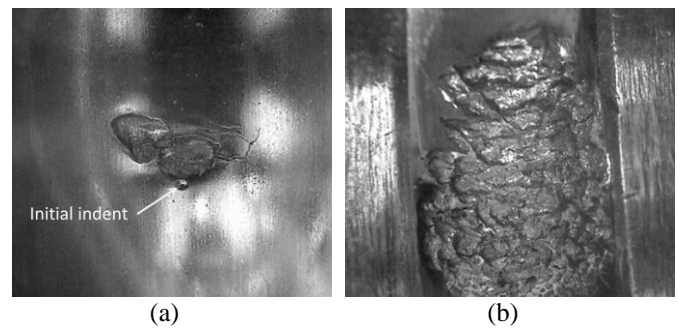

(a) (b)

Figure 4. Optical images taken from the two faulty ball bearings under tests: (a) with localized inner race fault, (b) with extended inner race fault. Note that both images have different magnification scales.

The realistic spall faults were induced on the bearings by means of accelerated life tests (ALTs) performed on a custom-made test rig (not discussed in detailed here). The ALT on each bearing was realized according to the

3

procedure described in Figure 5. First of all, a brand-new bearing is disassembled. Later on, the inner race of the bearing is indented with a Rockwell C indenter (the applied load is chosen such that the indent diameter is about 240 micron). After that, the bearing is reassembled and mounted to a dedicated test rig. The bearing is continuously run on the setup with a constant shaft speed of 1500 rpm and a constant radial load of 10 kN (~66% of dynamic rating load). Finally, the test is stopped until a pre-determined duration is attained.
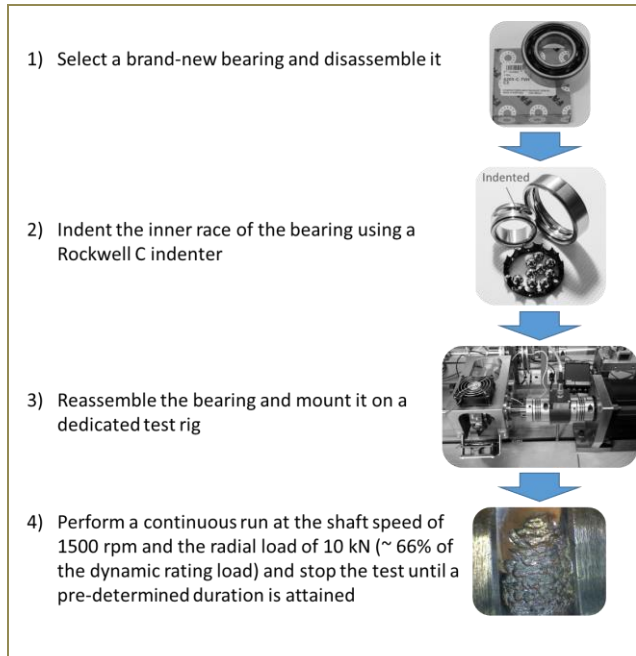

Figure 5. Procedure to create realistic spall faults in an accelerated way.

3.3. Design of Experiment

Three operational parameters, (1) shaft speed, (2) radial load and (3) bearing/oil temperature, that are typically time-varying in many applications were selected in this study. The range of each operational parameter was considered as industrially relevant as possible. Table 2 lists out the absolute and relative range of each operational parameter.

Operational parameter	Nominal value	Absolute variation	Relative variation
Shaft speed [rpm]	1050	600-1500	[-43%; +43%]
Radial load [N]	1500	750-2250	[-50%; +50%]]
Oil temperature [^{0}C]	45	30-55	[-33%; +22%]

Table 2. The range of the operational parameters considered in the experiment.

A custom Design of Experiment (DoE) for three factors publicly made available by (Brezani, 2014) was used to determine the number of tests for each bearing and the combinations of three operational parameters in each test

condition. In total, there were 41 conditions to be tested for each bearing. Note that the custom DoE is based on the Central Composite Design (CCD) (Montgomery, 1997), but with more levels for each factor. Figure 6 visualizes all the 41 test conditions distributed in the cubic space to be tested in each bearing.
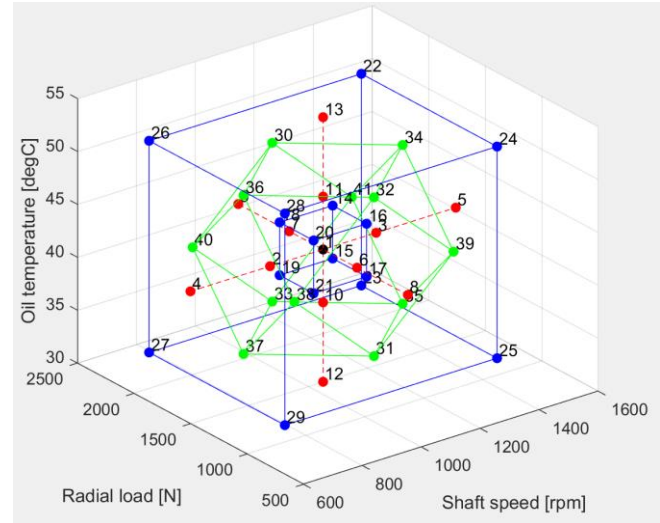

Figure 6. Visualization of the 41 operating conditions to be tested for each bearing. Note that each node denotes a test condition.

3.4. Test Procedure

After a bearing of interest (either healthy bearing or faulty bearing) is properly mounted on the setup shown in Figure 2, a test condition specified in Figure 6 was imposed by controlling the shaft speed, radial load and bearing temperature to the desired values. Once the steady state at each specified condition is achieved (i.e. by waiting for the setup to have run for about 1–2 minutes), the accelerometer signal is recorded for a duration of 10 seconds using a commercial data acquisition system. The digital data are then transmitted and stored into a PC for further analysis as will be discussed in the next section. This procedure is repeated for each bearing until all the specified test conditions are completed.

4. RESULTS AND DISCUSSION

The vibration signals acquired from all test conditions have been processed to compute the BPFI feature using the algorithm described in Section 2. As a benchmark, some traditional statistical features like (*i*) RMS, (*ii*) kurtosis, (*iii*) crest factor, (*iv*) peak-value and (*v*) peak-to-peak, have also been extracted from the raw vibration signals.

The *F-statistics* was used in this study for comparing the diagnostic performance of the BPFI feature with the traditional statistical features. This metric is defined as the ratio between *between-group variability* and *within-group*

variability Mathematically speaking, the *F-statistics* is formulated as follows (Lomax, 2007):

$$\text{F} - \text{statistics} = \frac{\text{between} - \text{group variability}}{\text{within} - \text{group variability}} \qquad (3)$$

where the *between-group variability* Var_{bg} is expressed as:

$$\text{Var}_{bg} = \frac{1}{K-1} \sum_{i=1}^{K} n_i (\bar{Y}_i - \bar{Y})^2 \qquad (4)$$

with $\bar{Y}_i$ denoting the sample mean of the *i*-th group, n_i denoting the number of observations in the *i*-th group, $\bar{Y}$ denoting the overall mean of the data, and K denoting the number of groups. Meanwhile, the *within-group variability* Var_{wg} is expressed as:

$$\text{Var}_{wg} = \frac{1}{N-K} \sum_{i=1}^{K} \sum_{j=1}^{n_i} n_i (Y_{ij} - \bar{Y}_i)^2 \qquad (5)$$

with Y_{ij} denoting the *j*-th observation in the *i*-th group out of K groups and N denoting the overall sample size.

Intuitively, the *F-statistics* expressed in the equation above can be seen as a metric describing a discriminating power (separation degree) between groups as illustrated in Figure 7. The higher the *F-statistics* value, the better the separation between groups will be.
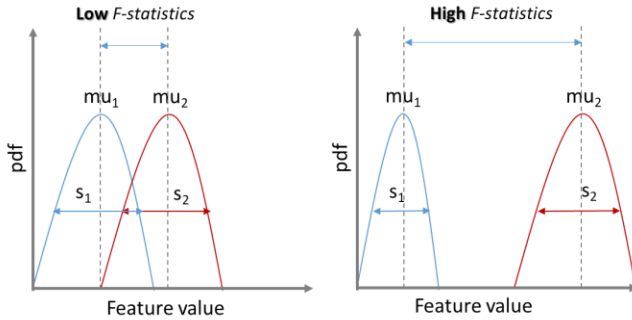

Figure 7. Graphical representation of the probability distribution functions (pdf) of two groups with low and high F-statistics

Figure 8 and Figure 9 show the boxplots labelled with the F-statistics of the BPFI feature and the crest factor feature from all test conditions, respectively. The boxplots of the other statistical features are not shown here because their F-statistics are lower than that of the crest factor as seen in Table 3. Hence, based on the calculated F-statistics shown in the figures and the table one may conclude that the BPFI feature outperforms the traditional statistical features (the F-statistics of the BPFI feature is the highest).
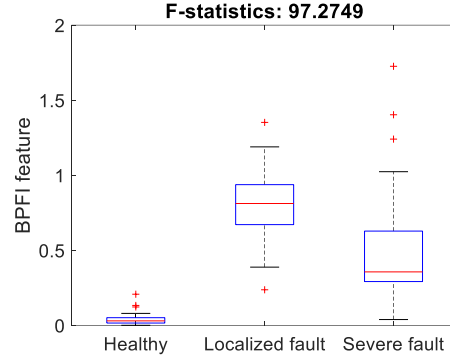

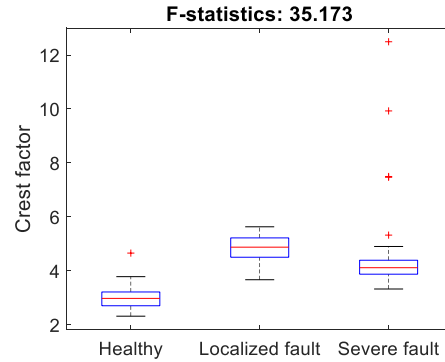Figure 8. Boxplot of the BPFI feature extracted from all the test conditions

Figure 9. Boxplot of the crest factor (CF) feature extracted from all the test conditions.

Notably, the global trends of the BPFI and crest factor feature with respect to the fault size are quite similar. Both the BPFI and crest factor feature values get higher when the localized fault occurs. Furthermore, when the fault progresses, both feature values decrease. A possible explanation for this observation is that localized faults occurring in bearing systems generates high-level impulsive excitations compared to extended faults (Randall & Antoni, 2011). Since the BPFI feature is a quantity expressing the impulsiveness degree for a specific inner race fault, while the crest factor feature is a quantity expressing the overall impulsiveness degree, as a result, the values of both features for the localized fault are higher compared to the healthy state and they get lower for the extended fault.

Traditional statistical feature	F-statistics
RMS	3.99
Kurtosis	6.16
Peak value	9.15
Peak-to-peak	9.64

Table 3. The F-statistics value of the other traditional statistical features.

Although the F-statistics for both the BPFI and crest factor features are relatively high, however one may still observe some overlapping between groups (i.e. bearing with different degradation level) in the boxplots. This overlapping may lead to false negative/false positive that will in turns affect a wrong diagnostic decision. As will be shown in the subsequent paragraphs, the overlapping is mainly caused by the variations in the operating conditions.
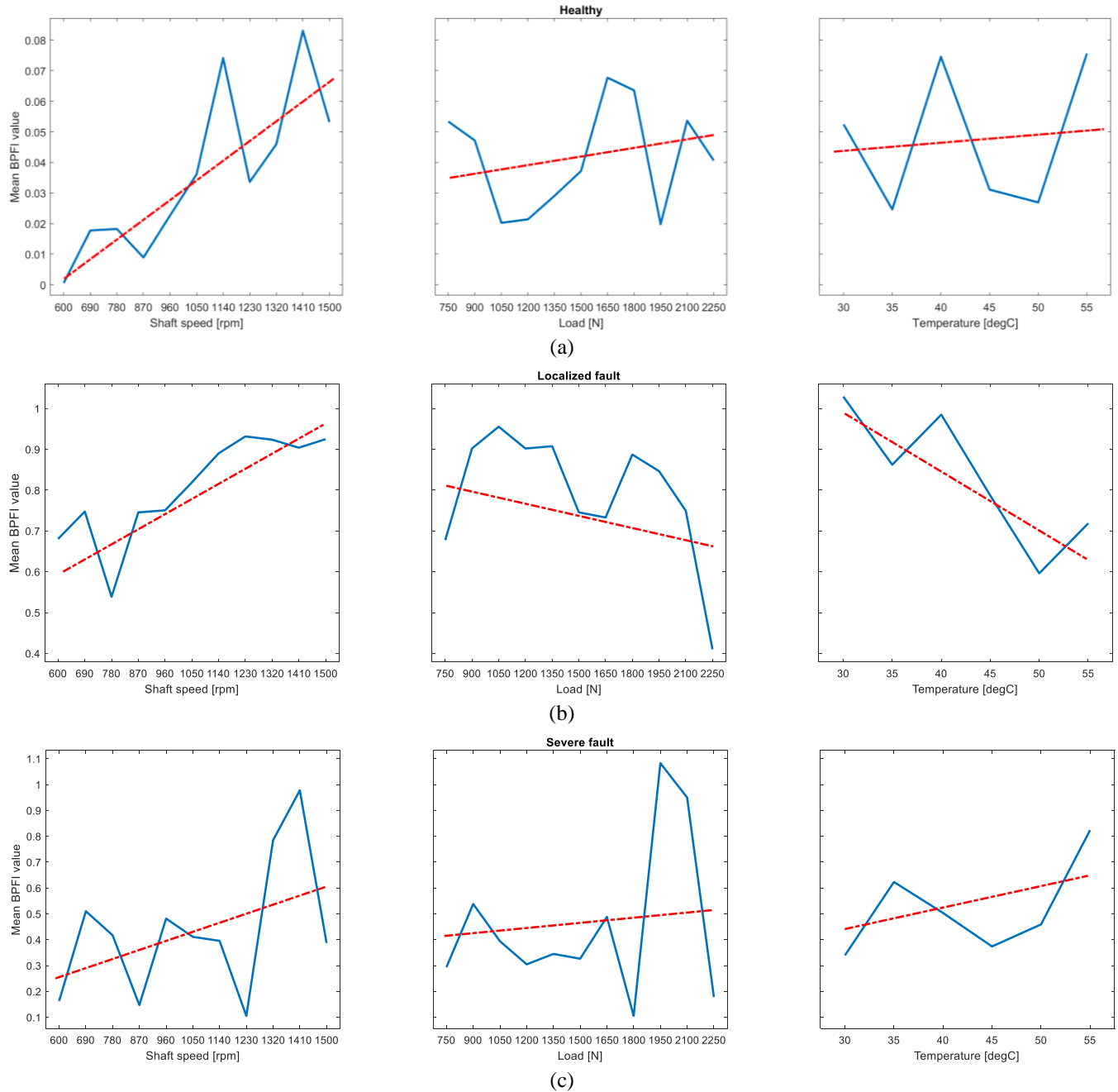

Figure 10. Visualization of the main effects of the three operational parameters, namely shaft speed, radial load and oil temperature, on the *BPFI feature* extracted from vibration signals measured in (a) healthy bearing, (b) bearing with localized inner race fault, (c) bearing with severe extended inner race fault.
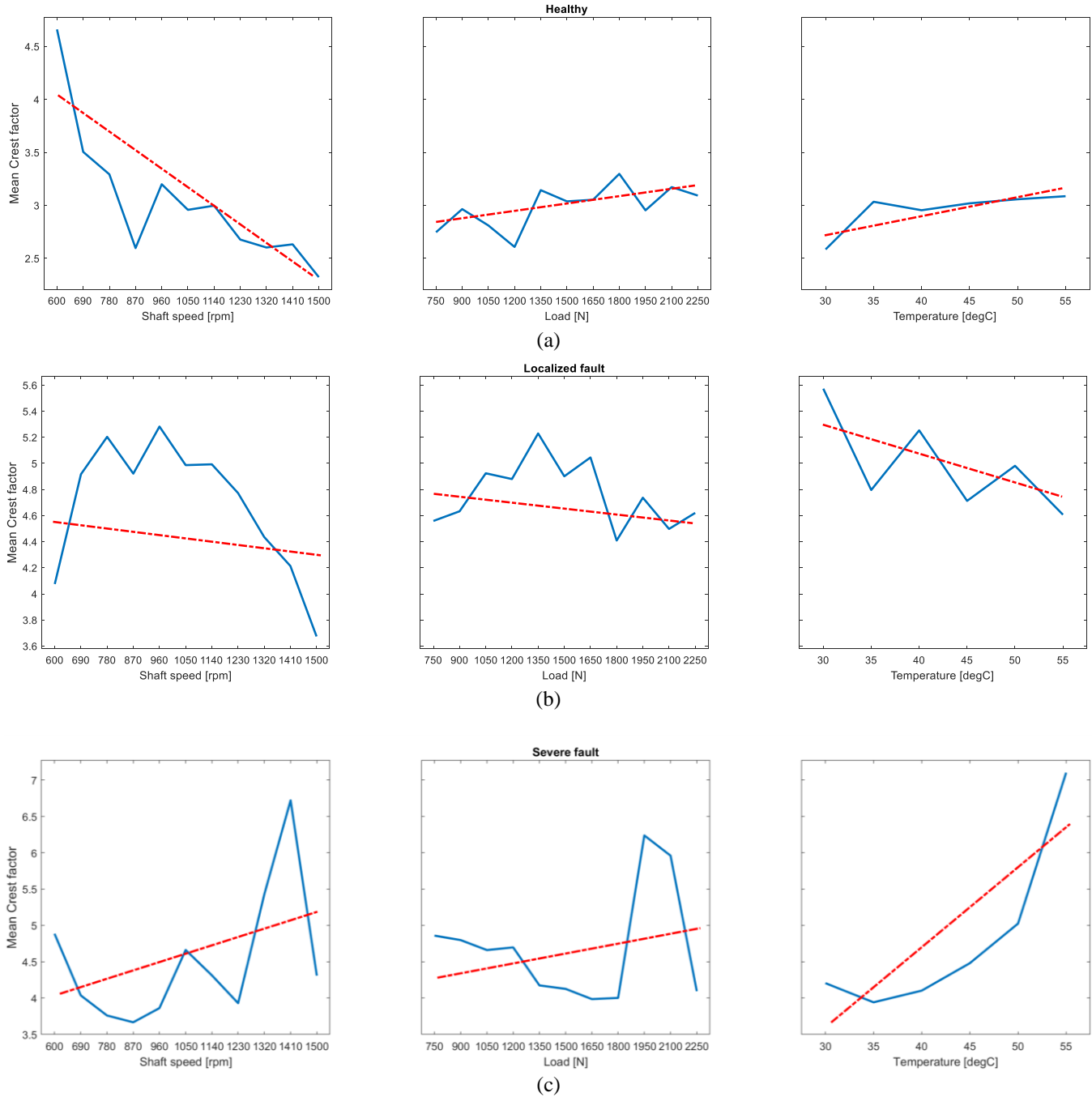
Figure 11. Visualization of the main effects of the three operational parameters, namely shaft speed, radial load and oil temperature, on the *Crest factor feature* extracted from vibration signals measured in (a) healthy bearing, (b) bearing with localized inner race fault, (c) bearing with severe extended inner race fault.

Figure 10 and Figure 11 show the effects of the shaft speed, radial load and bearing temperature variations on the BPFI and crest factor features, respectively. Both figures clearly show strong dependencies of the two features on the operating conditions. Moreover, the figures also show that there is a significant dependency of the feature values on the fault severity, which can be observed on the global trends (indicated by the dashed lines) between the feature values and the operating parameter. The overall trends of the features values in function of the operating conditions can be qualitatively summarized in Table 4 and Table 5. Note

that the sign (+) denotes a positive slope, while the sign (-) denotes a negative slope.

Severity level	Shaft speed	Load	Temperature
Healthy	(+)	(+)	(+)
Localized fault	(+)	(-)	(-)
Extended fault	(+)	(+)	(+)

Table 4. The overall dependencies of the *BPFI* feature on the operating parameters.

Severity level	Shaft speed	Load	Temperature
Healthy	(-)	(+)	(+)
Localized fault	(-)	(-)	(-)
Extended fault	(+)	(+)	(+)

Table 5. The overall dependencies of the *crest factor* feature on the operating parameters.

It is worth of mentioning here that the overall trends of both the BPFI and crest factor feature in function of bearing temperature are quite similar for different fault severity level. For localized fault, the BPFI and crest factor feature values decrease with increasing temperature. On the contrary, both feature values increase with increasing temperature for extended fault. This indicates that the fault geometry might affect the formation of the oil film thickness between the rolling element and the inner race that will eventually influence the bearing vibration response.

Both the BPFI and crest factor feature values decrease with increasing load for the localized fault. In contrast, the two feature values seem to increase with increasing load for the extended fault. It is not clear yet to the authors a possible explanation of this observation.

Besides the fault size, the impulsive excitation force caused by a defect in bearings is also dependent on the shaft speed (Choudhury & Tandon, 2005). At low shaft speeds, the resulting impulsive excitation force is small and is severely attenuated through the propagation from the excitation source (fault location) and the measuring points (accelerometer locations). In contrast, the resulting impulsive excitation at high speeds is large. As expected from this reasoning, the BPFI feature value increases with the increasing shaft speed for the three bearing conditions. However, the increasing trend in function of the shaft speed is not consistently observed on the crest factor feature.

5. CONCLUSION & PERSPECTIVES

The robustness of the envelope based feature for bearing fault detection against operating condition variations has been evaluated. As a benchmark, the robustness of some statistical features (RMS, kurtosis, peak-to-peak, peak value, and crest factor) against operating condition variations has also been evaluated. The performance of all the considered features was evaluated quantitatively by

means of the *F-statistics* metric. It turns out that the crest factor feature is the best feature out of the traditional statistical features for bearing fault detection. Nonetheless, the envelope based feature outperforms the crest factor feature in terms of a fault detection purposes.

Some overlapping between feature values extracted from different bearing states are still observed if the operating condition is not taken into account in the decision. In fact, this overlapping needs to be avoided because it leads to false negative/false positives. As already proposed by some authors in the literature (Bartelmus, & Zimroz, 2009; Zimroz et al., 2014), a relationship between a feature and operational parameters can be used to define new features or to normalize features for fault detection that are more robust against operating condition variations.

The main effects of operational parameters variations on the envelope based feature and the crest factor feature have been experimentally analyzed. It is shown that the operational parameters (shaft speed, radial load, bearing temperature) *significantly influence* both the envelope-based feature and the statistical features. The relationships between the feature values extracted from three different bearing states and the operational parameters (shaft speed, radial load, and bearing temperature) have been individually established. As discussed earlier, these relationships can be used to compute new features or to normalize the features such that they become robust (i.e. independent of operating conditions) for fault detection purposes.

However, modeling the relationships between the features and the operational parameters to define new features as discussed above seems to be unreliable approach for fault severity assessment and prognostics purposes. The reasoning of this conclusion is that the fault severity level also affects the relationships between the features and the operational parameters. This implies that unique models relating the features and the operational parameters cannot be built during the lifetime of bearings. Some future works that can be addressed to tackle the limitation of the presented features for bearing fault prognostics are as follows. The first possible approach is to develop a strategy using the presented features on how to define operating condition range in which the effects of operational parameters on the features are minimal. In this context, significant amount of data are needed, where one can benefit from fleet-data. The second possible approach that requires more fundamental research and significant effort is to define new bearing fault features to be extracted from vibration signals that are independent of operating condition variations.

REFERENCES

Barbini, L., Ompusunggu, A. P., Hillis, A. J., du Bois, J. L., Bartic, A., (2017), Phase editing as a signal pre-processing step for automated bearing fault detection. *Mechanical Systems and Signal Processing*, Vol. 91, pp. 407-421.

Bartelmus, W., & Zimroz, R., (2009), A new feature for monitoring the condition of gearboxes in non-stationary operating conditions, *Mechanical Systems and Signal Processing*, Vol. 23(5), pp. 1528-1534.

Boskoski, P., Juricic, D., & Stankovski, M., (2010), Gear and bearing fault detection under variable operating conditions, In the proceedings of the *Annual Conference of the Prognostics and Health Management Society*.

Brezani, I., (2014), GUI for evaluation of a custom three variables multilevel DOE, Matlab codes are available through: https://www.mathworks.com/matlabcentral/mlc-downloads/downloads/submissions/45837/versions/1/previews/html/Manual.html?access_key= (Updated 11th March 2014, Last viewed on 30th April 2018)

Choudhury A.A., & Tandon N.N., (2005), Vibration Response of Rolling Element Bearings in a Rotor Bearing System to a Local Defect Under Radial Load. *ASME. J. Tribol.*, Vol.128(2), pp. 252-261.

Gelman, L., Patel, T., Murray, B., & Thomson, A., (2013), Rolling Bearing Diagnosis Based on the Higher Order Spectra, *International Journal of Prognostics and Health Management*, ISSN 2153-2648, 022

Lomax, R. G. (2007), *Statistical Concepts: A Second Course*. ISBN 0-8058-5850-4.

Montgomery, D. C., (1997), *Design and analysis of experiments* (4th Ed.), New York: Wiley.

Ompusunggu, A. P., Bartic, T. A., (2016), Automated cepstral editing procedure (ACEP) for removing discrete components from vibration signals, *International Journal of Condition Monitoring*, Vol. 6, pp 56-61.

Randall, R. B. & Antoni, J., (2011), Rolling element bearing diagnostics-A tutorial. *Mechanical Systems and Signal Processing,* Volume 25, p. 485–520.

Zimroz, R., Bartelmus, W., Barszcz, T., & Urbanek,, J. (2014), Diagnostics of bearings in presence of strong operating conditions non-stationarity - A procedure of load-dependent features processing with application to wind turbine bearings, *Mechanical Systems and Signal Processing (MSSP), Vol. 46(1), pp.16-27.*

FAG. https://www.schaeffler.com/remotemedien/media/_shared_media/08_media_library/01_publications/schaeffler_2/tpi/downloads_8/tpi_165_de_en.pdf

BIOGRAPHIES

Agusmian P. Ompusunggu is a senior research engineer at Flanders Make vzw, Belgium. He has been working in R&D projects in the area of (*i*) development of PHM systems, (*ii*) structural dynamics/vibration analysis, (*iii*) industrial big data analytics, (*iv*) smart sensing, (*v*) material testing and characterization, (*vi*) contact mechanics & tribology, and (*vii*) additive manufacturing. He earned his bachelor degree in mechanical engineering (B.Eng) in 2004 and master degree in mechanical engineering (M.Eng) in 2006 both from Institut Teknologi Bandung (ITB), Indonesia. Later on, he pursued a PhD degree in mechanical engineering at the KU Leuven, Belgium, and obtained the PhD degree in 2012 with the focus on development of a condition monitoring and prognostics system for automatic transmissions.

Steven Devos is a project leader at Flanders Make vzw, Belgium. He led R&D projects a.o. in the area of noise and vibration and diagnostics. He earned his master degree in mechanical engineering (M.Eng) in 1999 at University Ghent. In 2006, he obtained a PhD degree in mechanical engineering at the KU Leuven (Belgium) on the development of an energy-efficient resonant piezoelectric motor.